Proceedings of the ASME/BATH 2015 Symposium on Fluid Power & Motion Control
FPMC2015
October 12-14, 2015, Chicago, Illinois, United States

FPMC2015-9606

CRANK-SLIDER SPOOL VALVE FOR SWITCH-MODE CIRCUITS

Alexander C. Yudell
PhD Student
Department of Mechanical Engineering
University of Minnesota
Minneapolis, MN, USA 55455
yudel004@umn.edu

Shaun E. Koktavy
MS Student
Department of Mechanical Engineering
University of Minnesota
Minneapolis, MN, USA 55455
kokta002@umn.edu

James D. Van de Ven
Assistant Professor
Department of Mechanical Engineering
University of Minnesota
Minneapolis, MN, USA 55455
vandeven@umn.edu

ABSTRACT
A key component of switch-mode hydraulic circuits is a high-speed two-position three-way valve with a variable duty cycle. This paper presents a new valve architecture that consists of two valve spools that are axially driven by crank-slider mechanisms. By phase shifting the two crank links, which are on a common crankshaft, the duty cycle of the valve is adjusted. The two spools split and re-combine flow such that two switching cycles occur per revolution of the crankshaft. Because the spools move in a near-sinusoidal trajectory, the peak spool velocities are achieved at mid-stroke where the valve land transitions across the ports, resulting in short valve transition times. The spool velocity is lower during the remainder of the cycle, reducing viscous friction losses. A dynamic model is constructed of this new valve operating at 120 Hz switching frequency in a switch-mode circuit. The model is used to illustrate design trade-offs and minimize energy losses in the valve. The resulting design solution transitions to the on-state in 5% of the switching period and the combined leakage and viscous friction in the valve dissipate 1.7% of the total power at a pressure of 34.5MPa and volumetric flow rate of 22.8L/min.

INTRODUCTION
Switch-mode hydraulics, analogous to switch-mode converters from the field of power electronics [1], is an emerging method of controlling hydraulic circuits. This concept utilizes a high-speed valve to switch between efficient on and off states, while temporarily storing energy in inductive and capacitive elements. The mean flow or pressure is controlled by the duty cycle, defined as the time in the on position divided by the switching period. Switch-mode hydraulics have been proposed for buck/boost converters [2], pumps [3-6], linear actuators [7], engine valves [8], and multiple actuators [9]. The benefits of this approach are low cost, low weight, good response time, and improved efficiency over throttling valve control [3, 9].

The valve in a switch-mode hydraulic circuit has a demanding set of competing requirements for the circuit to achieve good performance and high efficiency. A high performance circuit, defined by a fast response time and a low flow ripple, requires a fast valve switching frequency. However, a fast switching frequency creates three main challenges. First, high frequency valves typically use a low mass switching element to minimize the inertial actuation forces. The low mass typically correlates to a small flow area, requiring a balance between fully-open throttling loss and inertial force. Second, each switching event results in throttling across the partially-open transitioning valve. This energy loss can be minimized through soft switching [10, 11] or by reducing the valve transition time, at the expense of increasing the velocity of the switching element. Finally, each switching cycle incurs losses due to compressing and decompressing the fluid in the switched volume. The compressible energy loss can be minimized by reducing the switched volume between the valve and the inductive element.

While the switching frequency limit for off-the-shelf solenoid valves is around 10 Hz [12], multiple researchers are developing high-speed valves specifically for switch-mode circuits. High-speed valve designs reported in the literature include: solenoid valves [7, 13], poppet valves [14], linear spool valves [4, 15], and continuously rotating axial and radial flow valves [6, 16-20].

In this work, a novel high-speed valve for switch-mode control is presented. The objective of the new valve is to achieve a high switching frequency, a short valve transition, and an adjustable duty cycle in a valve architecture that can be easily constructed for experimental studies of switch-mode circuits. The new linkage-based valve architecture is presented in section 2, followed by the development of a model of the valve to act as a design guide in section 3. The results of the detailed design are presented in section 4, followed by a discussion and concluding remarks in section 5.

NOMENCLATURE

A_{eff}	Effective area of series orifices
A_o	Orifice Area
c	Radial clearance between spool and sleeve
C_d	Orifice discharge coefficient
D	Duty cycle of valve outlet 1
d_o	Orifice diameter
l	Couple link length
L	Instantaneous length of leakage path
N	Number of parallel orifices
Q	Volumetric flow rate
r	Crank link length
r_o	Orifice radius
v	Spool velocity
x	Spool axial displacement
x_n	Spool neutral position
x_o	Distance from spool land to open edge of orifice
ΔP	Pressure drop
θ	Crank link angular displacement
μ	Working fluid dynamic viscosity
ρ	Mass density of working fluid
ϕ	Phase shift between crank links
ω	Crank link angular velocity

DESIGN CONCEPT

The new three-way valve consists of two parallel spools, which act as the slider links of four-bar crank-slider mechanisms. A schematic of the valve architecture is presented in FIGURE 1. The spools S_1 and S_2 translate axially in the fixed valve housing, allowing connection of alternating ports in the housing. The spools are driven by a common crankshaft which ensures fixed relative position of the crank arms. The valve in FIGURE 1 is critically lapped, which is desirable to prevent crossporting while minimizing the time which the flow path is blocked.

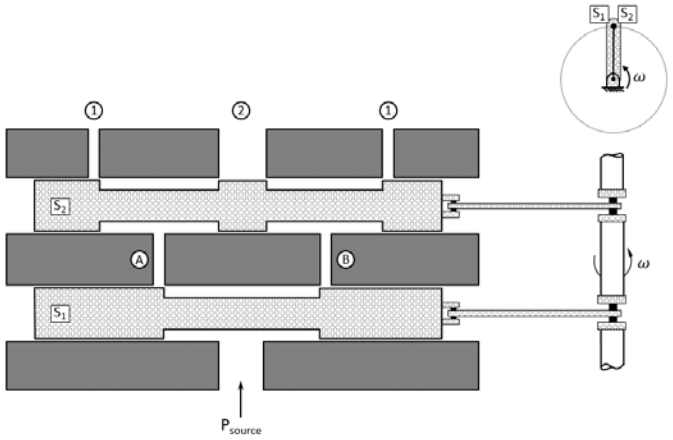

FIGURE 1. CRANK-SLIDER VALVE IN THE NEUTRAL POSITION.

The duty cycle of the valve is defined as ratio of time that the source is connected to outlet port 1 to switching period time. Valve duty cycles from 0 to 100% can be achieved by adjusting the phase angle between the spools from 0 to π radians. This phase shift modulation approach allows continuous adjustment of duty cycle and results in two switching cycles per revolution of the crank arm.

Spool S_1 switches the source flow between internal ports A and B, while spool S_2 alternates between connecting A to outlet port 1 and B to outlet 2 and vice versa. Both outlet ports labeled 1 would be connected either internally or externally to the valve, behaving as a single outlet. The axial location of a spool in the blocking position is referred to as the neutral position.

From the kinematics of a non-offset crank-slider mechanism, shown in FIGURE 2, the slider position is described by:

$$\boldsymbol{x(\theta) = r\sin\theta + l\sqrt{1-\left(\frac{r}{l}\cos\theta\right)^2} - \sqrt{l^2 - r^2}} \qquad (1)$$

where $x(\theta)$ is the displacement of the spool relative to the neutral position, r is the length of the crank link, l is the length of the coupler link, and θ is the angle of the crank arm with respect to the neutral position.
Differentiating the position with respect to time yields the velocity of the spool in terms of angular displacement of the crank, θ, relative to the vertical axis:

$$\boldsymbol{v(\theta) = r\omega\left(\cos\theta - \frac{r}{l}\frac{\sin\theta\cos\theta}{\sqrt{1-\left(\frac{r}{l}\cos\theta\right)^2}}\right)} \qquad (2)$$

where ω is the angular velocity of the crank link.

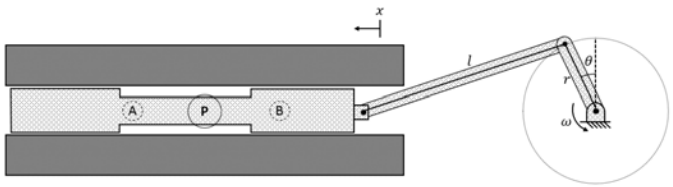

FIGURE 2. CRANK SLIDER VALVE ACTUATION MECHANISM. CRANK ANGLE IS MEASURED FROM THE NEUTRAL POSITION WHICH IS SHOWN WITH A DOTTED LINE.

When the length of the coupler link, *l*, is long relative to the crank link, *r*, the maximum absolute spool velocity occurs when the crank arm is perpendicular to the slider link travel, or $\theta = 0$ and $\theta = \pi$ with respect to the neutral position. As the valve transition time is dependent on the spool velocity during the port switching, the transition time is minimized by having the valve spool transition from one port to the other at the peak spool velocity. After transition, the spools decelerate to zero velocity at the ends of their travel. The nature of the slider link velocity profile accomplishes two design goals: 1) Transition at maximum spool velocity to minimize throttling losses and 2) Reduce velocity outside of transition periods to reduce frictional and viscous losses. A flywheel on the crankshaft stores kinetic energy when the spool is decelerating and releases the energy during spool acceleration.

There are multiple flow paths through the valve depending on the crank position and phase shift between the spools. FIGURE 3 demonstrates the flow path through the valve for a crank arm phase shift of ϕ radians, when spool S_1 is displaced by $\theta_1 = \frac{\pi}{2}$ radians. The flow path is through internal port A and then to outlet port 2. At this instance, internal port B is blocked, as a result there is no flow through either outlet port 1.

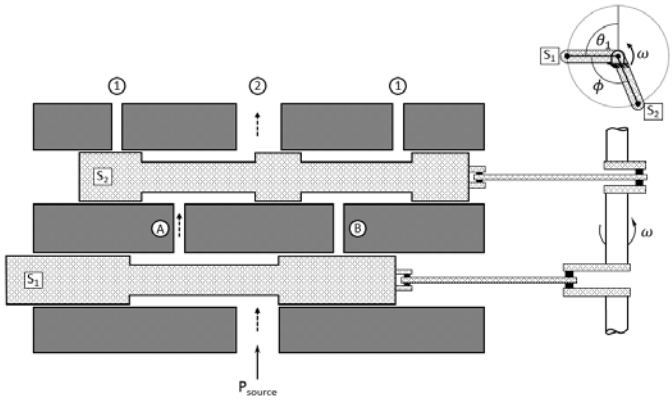

FIGURE 3. THE VALVE DEPICTED AT ANGULAR DISPLACEMENT $\theta_1 = \pi/2$ SHOWN IN THE SPOOL DISPLACEMENT PLOT OF FIGURE 4. SPOOLS ARE ϕ RADIANS OUT OF PHASE, WITH SPOOL S_1 $\pi/2$ RADIANS PAST THE NEUTRAL POSITION, AT MAXIMUM DISPLACEMENT. FLOW PATH IS INDICATED BY THE DOTTED ARROWS.

Continuous duty cycle adjustment can be achieved by phase shifting the crank angle of the valve spools. Figure 4 shows the valve displacements and resultant flow paths over a full crank rotation when, spool S_2 leads spool S_1 by the same ϕ radians shown in FIGURE 3. With reference to the 'Flow path Area' subplot, the flow is directed to outlet port 2 for a crank angular displacement equal to the ϕ radian phase shift.

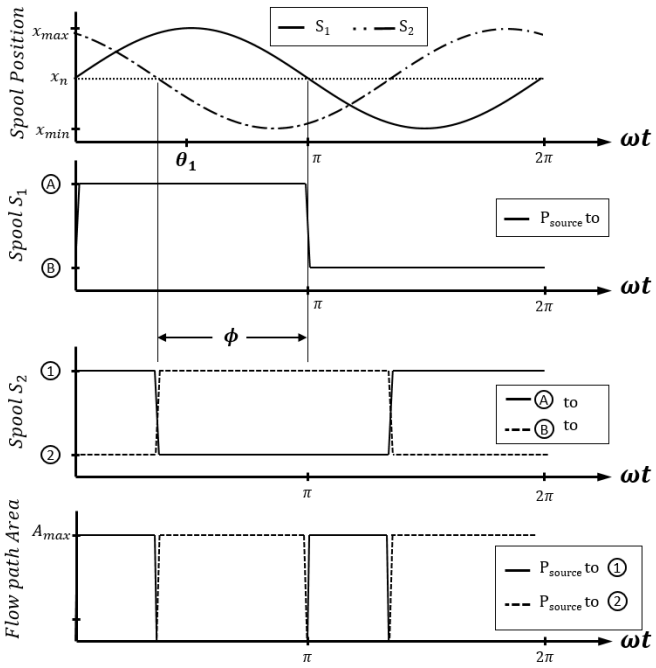

FIGURE 4. EXAMPLE OF HOW A PHASE SHIFT ϕ AFFECTS A DUTY CYCLE. x_n IN THE SPOOL POSITION PLOT REFERS TO THE SPOOL NEUTRAL POSITION. PORT LABELLING CONVENTION IS SHOWN IN FIGURES 1 AND 3.

The phase shift can be varied from 0 to π radians, resulting in outlet port 1 duty cycles described by:

$$D = \frac{\pi - \phi}{\pi} \qquad (3)$$

where *D* is the duty cycle of outlet port 1, and ϕ is the phase shift between the two spools. In a critically lapped valve with non-instantaneous transition, a duty cycle of 1 cannot be achieved due to each spool passing through a blocking state on each switching cycle. In this case, the duty cycle is reduced by the ratio of transition time to valve cycle time. The phase shift between the spools is achieved by rotating the crank arms relative to each other on the common crankshaft. In this design iteration, the crank arms are clamped to the crankshaft and the phase shift is adjusted offline. Future designs will have on line duty cycle adjustment capability. This can be achieved by linking the crank arms through a planetary gear train and adjusting the position of the carrier or with a variety of other mechanisms.

MODEL & DESIGN REQUIREMENTS

The objective of this design is to develop an energy efficient valve that can be used for experimental switch mode hydraulic circuit studies. The valve must have fast transition times with an adjustable duty cycle and operate at flows and pressures suitable for laboratory benchtop testing. An overview of defined constraints, design variables, and the desired objectives are presented in this section.

DESIGN CONSTRAINTS

The design flow rate and maximum pressure were selected as 22.8 liters/min and 34.5 MPa respectively, based on the capabilities of the available hydraulic power unit. The target pressure drop through the valve in the on-state at the rated flow is 345 kPa, which correlates to a 1% loss of the rated source pressure. The operating frequency of the valve is 120 Hz, which is be achievable by driving the crankshaft with a 3600rpm synchronous AC motor. This cyclic rate allows operation in the range of switching frequencies above and below the natural frequency of laboratory scale inertance tubes in a switched inertance hydraulic system topology [2].

The valve is determined to be in the 'on' state when the pressure drop across the active flow path is less than 345kPa at rated flow. The transition time is the time required to transition from a blocked state (orifices fully blocked) to the on-state. A transition ratio parameter is defined as the ratio of transition time to switching period. A transition ratio of 5% was selected to diminish transition throttling losses and allow for an absolute duty cycle of greater than 0.9 (based on two transition periods per valve switching period). This ratio is independent of the valve cyclic frequency and depends solely on valve and driving linkage geometry.

The valve uses a clearance seal between the spool and a ported sleeve. The sleeve has rows of radially drilled ports at the locations indicated in FIGURE 5, which are covered and uncovered by the lands on the spools. Ports distributed circumferentially around the sleeve balance the pressure and flow forces on the spool. In Fig. 5, the sleeve port rows are represented by a single orifice location. The sleeve fits into a valve housing containing the porting and O-ring seals. This design allows the low-mass sleeve to 'float' and thermally expand at a similar rate to the spool during startup to avoid binding. Additionally, using a sleeve makes manufacturing easier, as the precision ports can be drilled prior to sleeve installation.

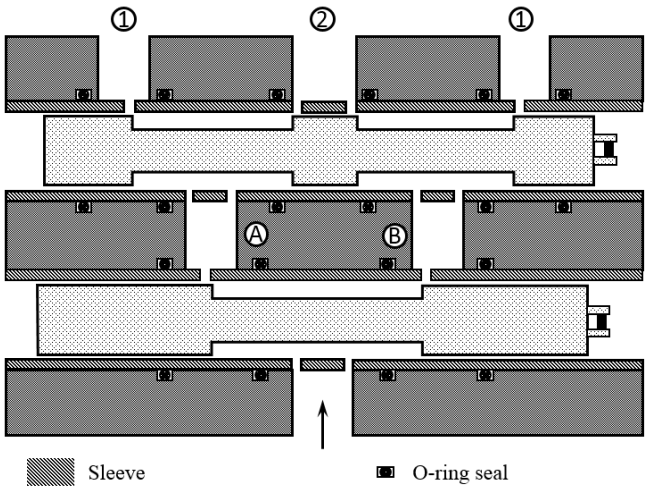

FIGURE 5. VALVE ILLUSTRATION SHOWING THE SLEEVE AND O-RING SEAL LOCATIONS. SLEEVE PORT LOCATIONS ARE REPRESENTED BY A SINGLE PORT.

The pressure drops through the valve were broken into primary and secondary losses. The primary losses consisted of the losses through the sleeve ports, which must be small in diameter for fast valve transition. The secondary pressure losses consisted of the pressure drops at inlet port, circumferential travel around the sleeve, and axial flow within in the spool grooves. The dimensions of the spool and porting within the housing were selected such that the secondary pressure drops are minor relative the pressure drops through the ports in the valve sleeve.

The pressure drop through each row of ports in the sleeve is described as:

$$\mathbf{\Delta P} = \frac{\rho}{2}\left(\frac{Q}{C_d A_o N}\right)^2 \quad (4)$$

where N is the total number of radial orifices in a row, ρ is the density of the hydraulic fluid, Q is the volumetric flow rate, C_d is the discharge coefficient and A_o is the open area of a single orifice.

During transition, the spool land covers or uncovers a row of circular ports. The area of the port orifices are a function of the axial spool position, as shown in FIGURE 6.

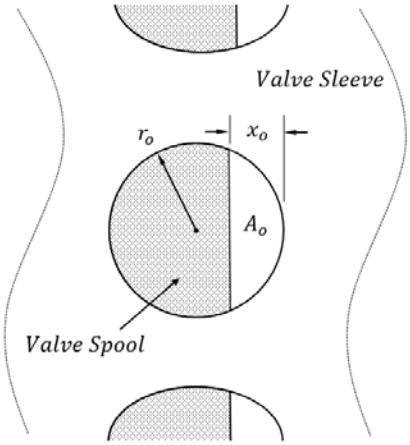

FIGURE 6. PORT ORIFICE AREA DURING VALVE TRANSITION.

The open area of an individual port is:

$$A_o = r_o^2 cos^{-1}\left(\frac{r_o - x_o}{r_o}\right) - (r_o - x_o)\sqrt{2r_o x_o - x_o^2} \quad (5)$$

where r_o is the port radius and x_o is the distance between the spool land (spool neutral position) and the open edge of the orifice.

With reference to FIGURE 5, each flow path contains 4 port orifice banks through which to pass, with the orifice areas designated A_1 closest to the source of flow through A_4 at the outlet. The port banks are in series, the pressure drop through the valve is equal to the sum of the pressure drop through each row of ports:

$$\Delta P = \frac{\rho Q^2}{2C_d^2}\left(\frac{1}{(A_1 N_1)^2} + \frac{1}{(A_2 N_2)^2} + \frac{1}{(A_3 N_3)^2} + \frac{1}{(A_4 N_4)^2}\right) \quad (6)$$

$$\Delta P = \frac{\rho Q^2}{2C_d^2 A_{eff}^2} \quad (7)$$

$$A_{eff} = \left(\frac{1}{(A_1 N_1)^2} + \frac{1}{(A_2 N_2)^2} + \frac{1}{(A_3 N_3)^2} + \frac{1}{(A_4 N_4)^2}\right)^{-0.5} \quad (8)$$

where A_{eff} is the effective area of the 4 series sleeve port locations. Orifice areas A_2 and A_4 are described by Eq. (5) during transition, while areas A_1 and A_3 are never blocked by the valve spool, so are the area of the circular ports. A_1 and A_3 can be composed of two rows of orifices to further reduce the pressure drop within the flow path, simplifying the effective area to:

$$A_{eff} = \left(\frac{2}{\left(\frac{\pi d_o^2}{4} 2N\right)^2} + \frac{1}{(A_2 N)^2} + \frac{1}{(A_4 N)^2}\right) \quad (9)$$

where A_2 and A_4 are described by Eq. (5) during transition.

Considering Eq. (6), the pressure drop across the valve is a function of the sleeve port open area and the number of sleeve orifices. When ΔP is less than 345kPa at 22.8L/min flow, the flow path is considered to be in the 'on' state. Based on the size and number of orifices, transition to the on-state may occur while ports are still partially blocked.

Equation 5 shows that A_2 and A_4 during transition are a function of the axial position of the valve spool. The velocity of the valve spool then dictates the time rate of change of pressure across a row of ports through Eq. (5) and (6) and hence the transition time. The velocity of the spool is most influenced by the crank length for a given input angular velocity as stated in Eq. (2).

The greatest pressure drop scenario occurs when both spools are in phase and moving through the neutral position. At this time, the port banks designated A_2 and A_4 are partially blocked simultaneously. A similar condition occurs when the spools are π radians out of phase. At other phase shifts, only one bank of ports transitions at a time. The analysis performed in the following section assumes that the spools are in phase.

Design Process

For ease of manufacturing, it was decided that the ports in a row should be spaced 30% of their diameter away from each other circumferentially based on their spacing at the inside wall of the sleeve. In this way, the inside circumference of the sleeve and thus diameter of the spool becomes a function of the number and diameter of ports in a particular row:

$$d_{spool} = \frac{1.3 N d_o}{\pi} \quad (10)$$

where d_{spool} is the diameter of the spool. As the number and diameter of sleeve ports increases, the pressure drop across the valve for a given spool position is decreased. Increasing N and d_o also increases the required diameter of the spool per Eq. (10) which comes at the cost of increased leakage flow through the clearance seal between the sleeve and the spool based on a parallel plate approximation of the annulus:

$$Q_{leak,pp} = \frac{\pi d_{spool} c^3 \Delta P}{12 \mu L_{leak}} = \frac{\pi d_{spool} c^3 \Delta P}{12 \mu\, x(\theta)} \quad (11)$$

where ΔP is the pressure difference between the pressurized flow and ambient, μ is the dynamic viscosity of the hydraulic fluid, and L_{leak} is the length of the leakage path. In all cases, the leakage flow was evaluated with $\Delta P = 34.5 MPa$. The value of c is limited by achievable machining tolerances.

The major leakage paths are between the valve ports within the spool as indicated in FIGURE 7 where the leakage path length, L_{leak} is the instantaneous axial displacement of the spool.

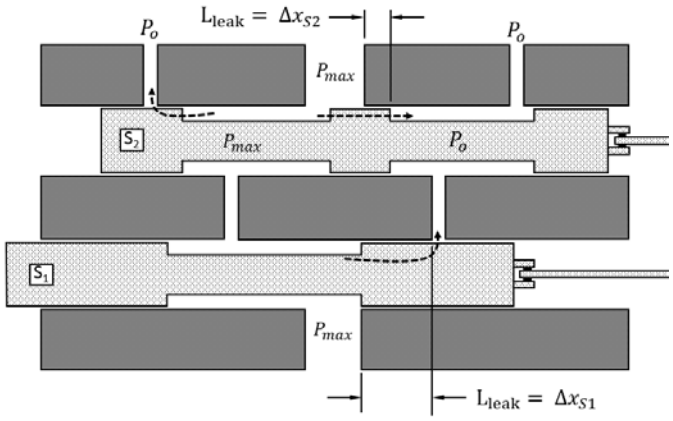

FIGURE 7. VALVE DIAGRAM SHOWING MAJOR LEAKAGE PATHS. THE LENGTH OF THE LEAKAGE PATHS ARE THE RESPECTIVE SPOOL DISPLACEMENTS RELATIVE TO THE NEUTRAL POSITION.

When a spool is at zero displacement, the leakage predicted by Eq. (11) would be infinite. To address this, the leakage flow model is switched to an orifice equation, based on the annular clearance area around the spool, once the flow predicted by the parallel plate leakage exceeds the flow predicted by the orifice model:

$$\boldsymbol{Q_{leak,o} = C_d A_{annulus}\sqrt{\frac{2\Delta P}{\rho}} = C_d(\pi d_{spool} c)\sqrt{\frac{2\Delta P}{\rho}}} \qquad (12)$$

Valve leakage to ambient is controlled by increasing the length of the lands at the ends of the spools. The length of the lands is penalized by increased viscous power dissipation in the fluid in the clearance between the spool and the sleeve. The viscous friction force is calculated with a parallel plate approximation of the annulus, and calculating the force from shear stress from Couette flow:

$$\boldsymbol{F_{vis} = -\pi d_{spool} L \mu \frac{v(\theta)}{c}} \qquad (13)$$

where F_{vis} is the viscous friction force and L is the total length of the spool lands.

MODELING

Modeling begins with the key valve requirement that a 345kPa on-state pressure drop that must be achieved within 5% of the valve switching cycle at the rated flow rate. The valve crank arms are powered by a 3600 rpm synchronous AC motor, yielding a constant angular crank velocity, $\omega = 120\pi$ rad/s. In order for the 5% transmission ratio to be met, transition to the on-state must occur prior to an angular crank displacement of $\pi * 0.05 = 0.157rad$ with respect to the neutral position.

Equation (1) yields an axial spool displacement for angular displacement in terms of crank length and coupler length. The *l*/*r* ratio of coupler length to crank link length is assumed to be 5 as a reasonable tradeoff between compactness and transmission angles. Rearranging Eq. (1) to solve for the spool displacement at 0.05π angular displacement and an *l*/*r* ratio of 5 yields:

$$\boldsymbol{x(0.05\pi) = 0.1589r} \qquad (14)$$

Equations (7) and (9) demonstrate that the pressure drop through the active flow path is a function of instantaneous sleeve port orifice areas and the number of port orifices.

At an angular crank displacement of 0.05π, the spool displacement described in Eq. (14) is the valve spool displacement (x_o) used to calculating the port open area A_2 and A_4 in Eq. (5). Thus, there is a minimum required crank length to achieve the 5% transition ratio for a given number and diameter of sleeve ports.

FIGURE 8 shows the required crank link length to achieve 5% transition for a range of port diameters and number of ports in an individual row.

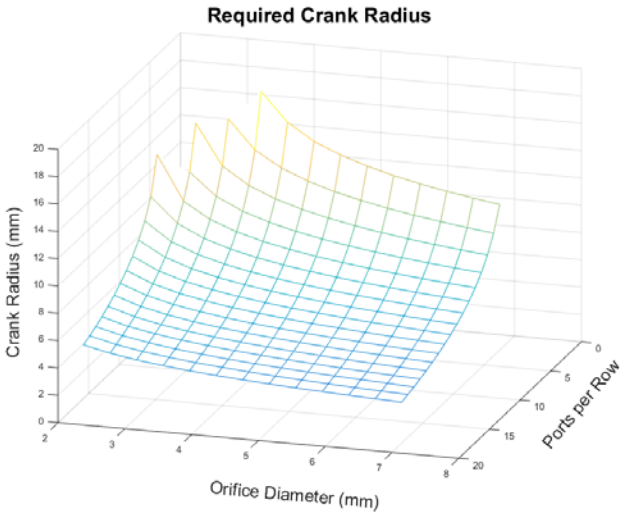

FIGURE 8. RELATIONSHIP BETWEEN THE NUMBER OF PORTS IN A ROW AND THE DIAMETER OF THE PORTS VS. THE REQUIRED CRANK LENGTH TO ACHIEVE A 5% TRANSITION RATIO.

The absolute value of the spool velocity over a cycle increases as crank length increases, per Eq. (2), resulting in higher viscous friction force given the same radial clearance between the spool and the sleeve, per Eq. (13). The clearance *c* can be increased to reduce the friction forces, but at the cost of increased leakage, per Eq. (11) and (12).

The energy loss over a cycle is the sum of the leakage and viscous friction losses:

$$\boldsymbol{E_{loss}} = \frac{\mathbf{1}}{\boldsymbol{\omega}}\int_0^{2\pi} \boldsymbol{\Delta P\, Q_{leak}(\theta)d\theta} + \frac{\mathbf{1}}{\boldsymbol{\omega}}\int_0^{2\pi} |\mathbf{F_{vis}}(\boldsymbol{\theta})\boldsymbol{v(\theta)}|\boldsymbol{d\theta} \quad (15)$$

where E_{loss} is the energy loss over a cycle due to leakage and viscous friction. The spool velocity, $v(\theta)$, is evaluated using Eq. (2). The energy loss for a given crank length is plotted in FIGURE 9 when spool land lengths are assumed to be 1.5*r.

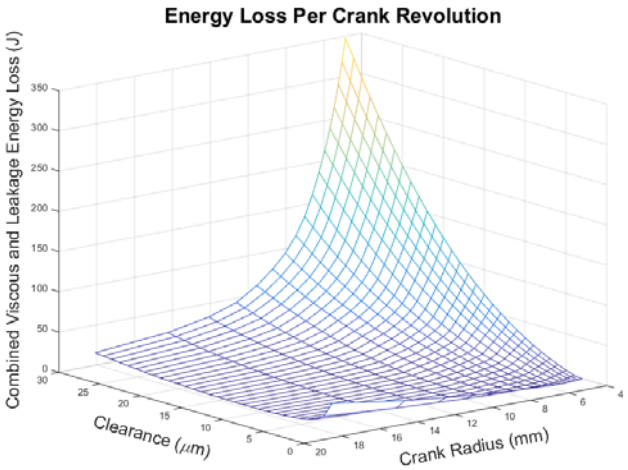

FIGURE 9. THE EFFECT OF CRANK LENGTH, AND RADIAL CLEARANCE, ON ENERGY LOSSES OVER A CYCLE.

FIGURE 9 indicates that clearances should be minimized until a clearance value of 2μm, at which value viscous friction becomes the major loss mechanism. The practical values of the radial clearance between the spool and sleeve are limited by manufacturing tolerance, and 10μm was selected as a minimum achievable value. As the valve lands increase in length, there is an increase in viscous forces per Eq. 12, but a reduction in leakage loss. FIGURE 10 illustrates this relationship, with a 10μm radial clearance applied.

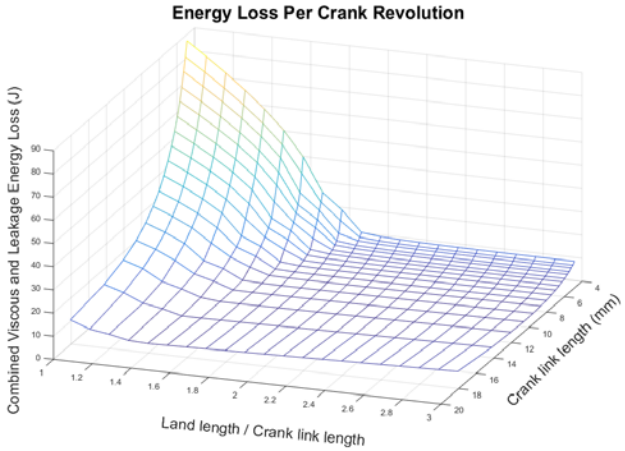

FIGURE 10. ENERGY LOSS OVER A CYCLE VS. THE CRANK LENGTH AND NONDIMENSIONALIZED SPOOL LAND LENGTH.

In FIGURE 10, the lowest per cycle losses are achieved for all crank link lengths when the spool land lengths are 2 times the length of the crank link. Energy loss as a function of crank length was then re-evaluated with a land length 2 times the crank length to find the optimal crank link length for a given radial clearance of 10μm as shown in FIGURE 11.

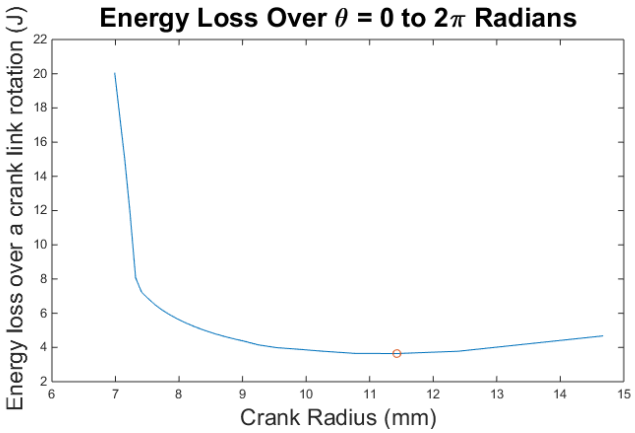

FIGURE 11. ENERGY LOSS OVER A CYCLE VS. CRANK LINK LENGTH, WITH OPTIMIZED LAND LENGTHS OF 2 TIMES THE CRANK LINK LENGTH AND A RADIAL CLEARANCE OF 10μm.

With reference to FIGURE 11, the optimal crank length that minimizes energy loss over a full crank rotation is 11.43mm. At short crank lengths, the leakage flow paths are small and leakage is the major loss mechanism. At long crank lengths, the viscous friction forces become the major loss mechanism.

The surface generated in FIGURE 8 is referenced to find the number of ports and port diameter required for transition ratio of 5% given the optimized crank length. Eight ports per row was selected to evenly distribute radial flow into the spool grooves, and for ease of manufacturing. With N = 8 ports per row, the required orifice diameter is 2.79mm.

RESULTS

The process outlined in the previous section resulted in an optimal crank length from which the sleeve port diameter was calculated, assuming 8 ports per row. TABLE 1 outlines the key design parameters of a slider valve which is capable of a 5% transition ratio at a rated flow of 22.8L/min and rated pressure of 34.5MPa.

TABLE 1: VALVE DESIGN OPTIMIZATION RESULTS

Attribute	Value
Orifice Diameter, d_o	2.79mm
Num. of Orifice, N	8 (outlet row, A_2, A_4) 8 x 2 rows (inlet row, A_1, A_3)
Crank Length, r	11.43mm
Spool Diameter, d_{spool}	9.23mm
Radial Spool Clearance, c	10μm

The effective area of the two outlet flow paths vs. crank link displacement at spool phase shift, $\phi = \frac{\pi}{2}$ is shown in FIGURE 12. The dashed horizontal line in the figure indicates the effective area that results in a pressure drop of 345kPa through the active flow path. The transition ratio is calculated as the time for an active flow path to achieve this effective area, divided by the valve switching frequency. For this optimized geometry, the transition ratio is 5.0%.

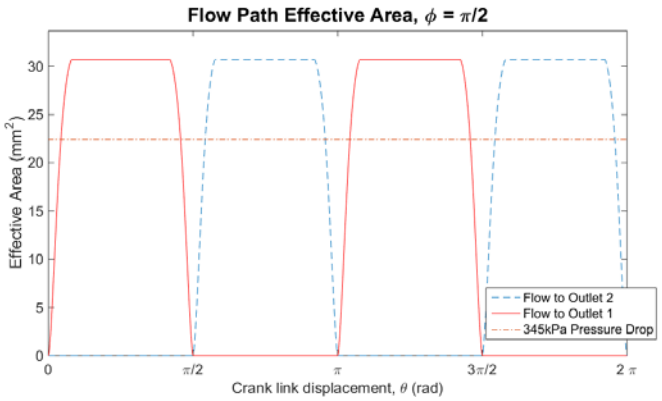

FIGURE 12. EFFECTIVE AREA OF THE VALVE VS. CRANK LINK DISPLACEMENT WHEN $\phi = \frac{\pi}{2}$.

The leakage and viscous friction losses are displayed as a fraction of the power at the rated flow and pressure in FIGURE 13. The peak values of leakage loss occur at the neutral point which is where the shortest leakage paths occur, generating the large increases in power loss at 0 and π crank angles. The viscous friction losses are proportional to the axial velocity of the spool but are small compared to the leakage losses. When integrated over 2π radians of crank displacement at an angular velocity of 120π radians per second, the energy loss due to leakage and viscous friction is 1.7% of rated flow energy over the same time.

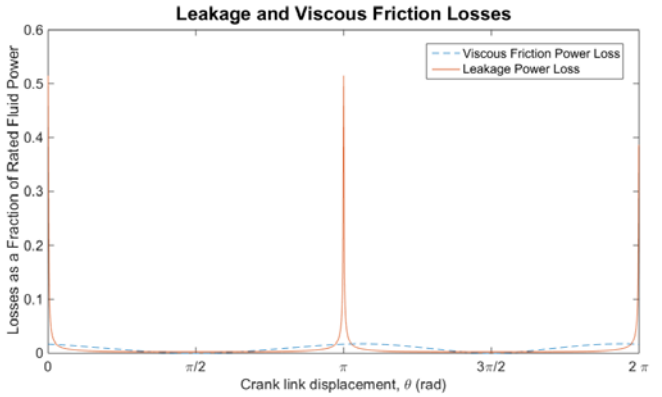

FIGURE 13. POWER LOSSES AS A FRACTION OF FLOW POWER AT RATED PRESSURE AND VOLUMETRIC FLOW RATE

A solid model of the valve design can be seen in FIGURE 14. The valve block is constructed of aluminum and the sleeve and spool are constructed from steel. The spool has a lower hardness than the sleeve and is the wear component during startup. It is desirable to have the spool and cylinder expand equally as they come up to operating temperature during startup to avoid binding. As the block has significantly more thermal mass and will not expand as quickly during warmup, a low-mass sleeve is utilized that expands with the spool. Adjacent orifices are separated by O-rings installed in the block. The inlet and outlet ports are located in the top of the valve block, on the far face of the housing as oriented in FIGURE 14. The ports in the valve housing are annular grooves, which allow the flow to enter the circumferentially distributed sleeve ports. Both ends of the spool are exposed to ambient, which pressure balances the valve. In this design iteration, leakage flows to ambient and is collected in a reservoir.

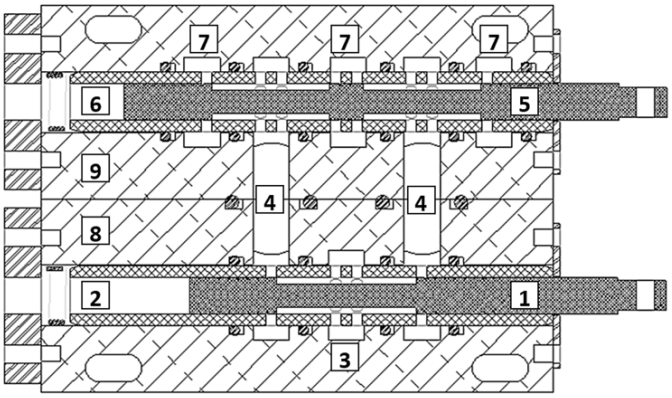

FIGURE 14. SOLID MODEL OF SPOOLS AND VALVE HOUSING

CONCLUSIONS & NEXT STEPS

The crank-slider-driven 3-way high-speed valve presented in this paper enables experimental studies of switch-mode hydraulic circuits at the frequencies required to achieve fast response, good control bandwidth, and reasonable inertance tube lengths for switched inertance converter circuits. Furthermore, the mechanical coupling to the valve makes the open area of the valve known at all times by measuring the crank angle, allowing easy comparison to numerical simulations. The valve was optimized for a given rated pressure of 34.5MPa and volumetric flow rate of 22.8L/min. The resulting valve is capable of transitioning to the on-state in 5% of the switching period, where the on state is defined as a pressure drop of 345kPa or less at the rated flow. The optimization process minimized the combined leakage and viscous friction losses on the sliding spool over a crank rotation, yielding a 1.7% energy loss relative to the flow energy over a cycle in the highest loss operating scenario.

Additional losses are incurred in switch-mode hydraulic circuits, including throttling across the valve and flow resistances. As these are highly dependent on the specific circuit architecture, they are not presented here but will be studied computationally and experimentally in future work.

The two spool design was investigated in this paper which allowed two cycles per revolution, but there is the potential of increasing the number of cycles per revolution by developing a valve of similar architecture which transitions at $\pi/4$, $3\pi/4$, $5\pi/4$ and $7\pi/4$ radians, compared to the present design which transitions at π and 2π radians. This would allow for four valve cycles per crank-shaft revolution at the expense of lower axial transition velocity.

REFERENCES

[1] Mohan, N., Robbins, W. P., and Undeland, T. M., 1995, Power Electronics: Converters, Applications and Design, Wiley and Sons, New York.

[2] Pan, M., Johnston, N., Plummer, A., Kudzma, S., and Hillis, A., 2014, "Theoretical and experimental studies of a switched inertance hydraulic system," Proceedings of the Institution of Mechanical Engineers, Part I: Journal of Systems and Control Engineering, 228(1), pp. 12-25.

[3] Li, P. Y., Li, C. Y., and Chase, T. R., 2005, "Software Enabled Variable Displacement Pumps," ASME International Mechanical Engineering Congress and Exposition, Orlando, FL, 12, pp. 63-72.

[4] Rannow, M. B., Tu, H. C., Li, P. Y., and Chase, T. R., "Software Enabled Variable Displacement Pumps- Experimental Studies," Proc. ASME International Mechanical Engineering Congress and Exposition.

[5] Tomlinson, S. P., and Burrows, C. R., 1992, "Achieving a Variable Flow Supply by Controlled Unloading of a Fixed-Displacement Pump," Journal of Dynamic Systems, Measurement, and Control, 114, pp. 166-171.

[6] Tu, H. C., Rannow, M., Van de Ven, J., Wang, M., Li, P., and Chase, T., 2007, "High Speed Rotary Pulse Width Modulated On/Off Valve," Proceedings of the ASME International Mechanical Engineering Congress, Seattle, WA, p. 42559.

[7] Muto, T., Yamada, H., and Suematsu, Y., 1990, "PWM-Digital Control of a Hydraulic Actuator Utilizing Two-Way Solenoid Valves," Journal of Fluid Control, 20(2), pp. 24-41.

[8] Lumkes, J. H., van Doorn, W., and Donaldson, J., 2005, "The Design and Simulation of a High Force Low Power Actuation System for Camless Engines," ASME International Mechanical Engineering Congress and Exposition, Orlando, FL, pp. 553-561.

[9] Beachley, N. H., and Fronczak, F. J., 1988, "A High Efficiency Multi-Circuit Sequential Apportioning Hydraulic System," National Conference on Fluid Power, Chicago, IL, pp. 141-152.

[10] Rannow, M. B., and Li, P. Y., 2012, "Soft Switching Approach to Reducing Transition Losses in On/Off Hydraulic Valve," Journal of Dynamic Systems, Measurement and Control (in press).

[11] Beckstrand, B., and Van de Ven, J. D., "Experimental Validation of a Soft Switch for a Virtually Variable Displacement Pump," Proc. ASME/BATH 2014 Symposium on Fluid Power & Motion Control, pp. FPMC2014-7857.

[12] Van de Ven, J. D., 2013, "On Fluid Compressibility in Switch-Mode Hydraulic Circuits - Part II: Experimental Results," Journal of Dynamic Systems, Measurement, and Control, 135(2), p. 021014.

[13] Kajima, T., Satoh, S., and Sagawa, R., 1994, "Development of a high speed solenoid valve," Transactions of the Japan Society of Mechanical Engineering: Part C, 60(576), pp. 2744-2751.

[14] Yokota, S., and Akutu, K., 1991, "A Fast-Acting Electro-Hydraulic Digital Transducer," JSME International Journal, 34(4), pp. 489-495.

[15] Cui, P., Burton, R. T., and Ukrainetz, P. R., 1991, "Development of a High Speed On/Off Valve," SAE Technical Paper Series(911815), pp. 21-25.

[16] Cyphelly, I., and Langen, H. J., 1980, "Ein neues energiesparendes Konzept der Volumenstromdosierung mit Konstantpumpen," Aachener Fluidtechnisches Kolloquium, pp. 42-61.

[17] Katz, A., and Van de Ven, J. D., 2009, "Design of a High-Speed On-Off Valve," International Mechanical Engineering Congress and Exposition, Lake Buena Vista, FL, 11189, pp. 1-10.

[18] Royston, T., and Singh, R., 1993, "Development of a Pulse-Width Modulated Pneumatic Rotary Valve for Actuator Position Control," Journal of Dynamic Systems, Measurement, and Control, 115, pp. 495-505.

[19] Van de Ven, J. D., and Katz, A., 2011, "Phase-Shift High-Speed Valve for Switch-Mode Control," Journal of Dynamic Systems, Measurement, and Control, 133(1).

[20] Wu, J., and Van de Ven, J. D., 2010, "Development of a High-Speed On-Off Valve for Switch-Mode Control of Hydraulic Circuits with Four-Quadrant Control," ASME International Mechanical Engineering Congress & Exposition, Vancouver, British Columbia, 37380.